

CONTENTS

Aquatic environment

- Speciation of organic phosphorus in a sediment profile of Lake Taihu I: Chemical forms and their transformation
Di Xu, Shiming Ding, Bin Li, Xiuling Bai, Chengxin Fan, Chaosheng Zhang 637
- Flow field and dissolved oxygen distributions in the outer channel of the Orbal oxidation ditch by monitor and CFD simulation
Xuesong Guo, Xin Zhou, Qiuwen Chen, Junxin Liu 645
- Removal of Cu(II) from acidic electroplating effluent by biochars generated from crop straws
Xuejiao Tong, Renkou Xu 652
- Optimisation of chemical purification conditions for direct application of solid metal salt coagulants:
Treatment of peatland-derived diffuse runoff
Elisangela Heiderscheidt, Jaakko Saukkoriipi, Anna-Kaisa Ronkanen, Bjørn Kløve 659
- Removal of nitrogen from wastewater with perennial ryegrass/artificial aquatic mats biofilm combined system
Chongjun Chen, Rui Zhang, Liang Wang, Weixiang Wu, Yingxu Chen 670
- Microbial community characterization, activity analysis and purifying efficiency in a biofilter process
Hong Xiang, Xiwu Lu, Lihong Yin, Fei Yang, Guangcan Zhu, Wuping Liu 677
- Performance of a completely autotrophic nitrogen removal over nitrite process for treating wastewater with different substrates at ambient temperature
Xiaoyan Chang, Dong Li, Yuhai Liang, Zhuo Yang, Shaoming Cui, Tao Liu, Huiping Zeng, Jie Zhang 688
- Performance study and kinetic modeling of hybrid bioreactor for treatment of bi-substrate mixture of phenol-*m*-cresol in wastewater: Process optimization with response surface methodology
Sudipta Dey, Somnath Mukherjee 698
- Analysis of aerobic granular sludge formation based on grey system theory
Cuiya Zhang, Hanmin Zhang 710
- Ethyl thiosemicarbazide intercalated organophilic calcined hydrotalcite as a potential sorbent for the removal of uranium(VI) and thorium(IV) ions from aqueous solutions
T. S. Anirudhan, S. Jalajamony 717

Atmospheric environment

- Observed levels and trends of gaseous SO₂ and HNO₃ at Mt. Waliguan, China: Results from 1997 to 2009
Weili Lin, Xiaobin Xu, Xiaolan Yu, Xiaochun Zhang, Jianqing Huang 726
- Influence of SO₂ in incineration flue gas on the sequestration of CO₂ by municipal solid waste incinerator fly ash
Jianguo Jiang, Sicong Tian, Chang Zhang 735
- Seasonal variation and source apportionment of organic and inorganic compounds in PM_{2.5} and PM₁₀ particulates in Beijing, China
Xingru Li, Yuesi Wang, Xueqing Guo, Yingfeng Wang 741
- Emissions of particulate matter and associated polycyclic aromatic hydrocarbons from agricultural diesel engine fueled with degummed, deacidified mixed crude palm oil blends
Khamphe Phoungthong, Surajit Tekasakul, Perapong Tekasakul, Gumpon Prateepchaikul, Naret Jindapetch, Masami Furuuchi, Mitsuhiko Hata 751
- Ground-high altitude joint detection of ozone and nitrogen oxides in urban areas of Beijing
Pengfei Chen, Qiang Zhang, Jiannong Quan, Yang Gao, Delong Zhao, Junwang Meng 758

Environmental biology

- Characterization of *Methylocystis* strain JTA1 isolated from aged refuse and its tolerance to chloroform
Tiantao Zhao, Lijie Zhang, Yunru Zhang, Zhilin Xing, Xuya Peng 770
- Allelopathic effects of gallic acid from *Aegiceras corniculatum* on *Cyclotella caspia*
Yu Liu, Fei Li, Qixin Huang 776

Environmental health and toxicology

Toxicity detection of sodium nitrite, borax and aluminum potassium sulfate using electrochemical method

Dengbin Yu, Daming Yong, Shaojun Dong 785

Environmental catalysis and materialsA comparative study of Mn/CeO₂, Mn/ZrO₂ and Mn/Ce-ZrO₂ for low temperature selective catalytic reduction of NO with NH₃ in the presence of SO₂ and H₂O (**Cover story**)

Boxiong Shen, Xiaopeng Zhang, Hongqing Ma, Yan Yao, Ting Liu 791

Removal of benzotriazole by heterogeneous photoelectro-Fenton like process using ZnFe₂O₄ nanoparticles as catalyst

Junfeng Wu, Wenhong Pu, Changzhu Yang, Man Zhang, Jingdong Zhang 801

Metal loaded zeolite adsorbents for hydrogen cyanide removal

Ping Ning, Juan Qiu, Xueqian Wang, Wei Liu, Wei Chen 808

Preparation and evaluation of Zr-β-FeOOH for efficient arsenic removal

Xiaofei Sun, Chun Hu, Jiuhui Qu 815

Application of red mud as a basic catalyst for biodiesel production

Qiang Liu, Ruirui Xin, Chengcheng Li, Chunli Xu, Jun Yang 823

Amino-functionalized core-shell magnetic mesoporous composite microspheres for Pb(II) and Cd(II) removal

Yulin Tang, Song Liang, Juntao Wang, Shuili Yu, Yilong Wang 830

Electrochemical detection and degradation of ibuprofen from water on multi-walled carbon nanotubes-epoxy composite electrode

Sorina Motoc, Adriana Remes, Aniela Pop, Florica Manea, Joop Schoonman 838

Serial parameter: CN 11-2629/X*1989*m*211*en*P*25*2013-4



A comparative study of Mn/CeO₂, Mn/ZrO₂ and Mn/Ce-ZrO₂ for low temperature selective catalytic reduction of NO with NH₃ in the presence of SO₂ and H₂O

Boxiong Shen*, Xiaopeng Zhang, Hongqing Ma, Yan Yao, Ting Liu

College of Environmental Science and Engineering, Nankai University, Tianjin 300071, China

Received 27 July 2012; revised 13 September 2012; accepted 25 September 2012

Abstract

Ce-ZrO₂ is a widely used three-way catalyst support. Because of the large surface area and excellent redox quality, Ce-ZrO₂ may have potential application in selective catalytic reduction (SCR) systems. In the present work, Ce-ZrO₂ was introduced into a low-temperature SCR system and CeO₂ and ZrO₂ supports were also introduced to make a contrastive study. Mn/CeO₂, Mn/ZrO₂ and Mn/Ce-ZrO₂ were prepared by impregnating these supports with Mn(NO₃)₂ solution, and have been characterized by N₂-BET, XRD, TPR, TPD, XPS, FT-IR and TG. The activity and resistance to SO₂ and H₂O of the catalysts were investigated. Mn/Ce-ZrO₂ and Mn/CeO₂ were proved to have better low-temperature activities than Mn/ZrO₂, and yielded 98.6% and 96.8% NO conversion at 180°C, respectively. This is mainly because Mn/Ce-ZrO₂ and Mn/CeO₂ had higher dispersion of manganese oxides, better redox properties and more weakly adsorbed oxygen species than Mn/ZrO₂. In addition, Mn/Ce-ZrO₂ showed a good resistance to SO₂ and H₂O and presented 87.1% NO conversion, even under SO₂ and H₂O treatment for 6 hours, and the activity of Mn/Ce-ZrO₂ was almost restored to its original level after cutting off the injection of SO₂ and H₂O. This was due to the weak water absorption and weak sulfation process on the surface of the catalyst.

Key words: low temperature; selective catalytic reduction; manganese; Ce-ZrO₂; SO₂ poisoning

DOI: 10.1016/S1001-0742(12)60109-0

Introduction

Selective catalytic reduction (SCR) of NO with NH₃ in the presence of oxygen is widely used to reduce NO production in combustion processes due to its low cost and high efficiency (Kašpar et al., 2003). The commonly adopted commercial catalyst is V₂O₅-WO₃(MoO₃)/TiO₂, and its working temperature must be in the 300–400°C range (Broer and Hammer, 2000; Choo et al., 2003) in order to attain good catalytic activity and avoid pore plugging from the deposition of ammonium sulfate on the catalyst surface. Consequently, in order to avoid reheating the flue gas, the SCR catalyst unit must be located upstream of the desulfurizer and electrostatic precipitator. However, the high concentration of dust reduces the performance and longevity of catalysts. Therefore, it is necessary to develop low-temperature SCR catalysts which can be located downstream of the desulfurizer and electrostatic precipitator. Most flue gas contains small amounts of SO₂ even after the desulfurizer. Catalysts for low-temperature SCR

are generally very sensitive to SO₂ and can be deactivated by direct reaction between SO₂ and a component of the catalyst or by deposition of ammonia sulfate on the catalyst surface (Casapu et al., 2009; Zhu et al., 2000; Kijlstra et al., 1998). Furthermore, the deactivation activity of SO₂ will be more intense when H₂O is present (Huang et al., 2002). Catalyst deactivation by SO₂ and H₂O needs to be considered.

Many transition metal oxides have been used to improve the low-temperature activity. Among these metal oxides, manganese oxides have attracted special attention, due to their various types of labile oxygen which can complete the catalytic cycle, resulting in a significant enhancement of catalytic activity at low temperature (Wallin et al., 2004; Smirniotis et al., 2001; Chen et al., 2012). Various Mn-base catalysts such as MnO_x/TiO₂ (Qi and Yang, 2003; Pena et al., 2004), MnO_x/Al₂O₃ (Kijlstra et al., 1997) and MnO_x/AC (Marban and Fuertes, 2001; Tang et al., 2007) have been prepared and tested, and they showed various levels of catalytic activity under different conditions. In some reports, CeO₂ has been used to improve the SCR

* Corresponding author. E-mail: shenbx@nankai.edu.cn

activity and the resistance to SO₂ of catalysts (Reddy et al., 2003; Baidya et al., 2009; Shen et al., 2011). However, the surface area of CeO₂ is not large enough and its redox quality needs to be improved (Zhang et al., 2011). Ce-ZrO₂ is a widely used three-way catalyst support (Fornasiero et al., 1995). It has been reported that Zr can modify the catalyst surface area (Chary et al., 2006) and the insertion of Zr into the ceria lattice can improve the lattice oxygen mobility, resulting in a better redox quality (Liu et al., 2009). Therefore, there is reason to believe that Ce-ZrO₂ supports may have good performance in SCR catalytic systems.

In this article, a Ce-ZrO₂ support is introduced into the low-temperature SCR catalytic system to support manganese oxides. CeO₂ and ZrO₂ supports are also used to make a contrastive study. Mn/Ce-ZrO₂ and Mn/CeO₂ showed better activities than Mn/ZrO₂; and Mn/Ce-ZrO₂ showed better resistance to SO₂ and H₂O than Mn/CeO₂ and Mn/ZrO₂ in a 6-hr sulfur tolerance test. The reason for the better resistance of Mn/Ce-ZrO₂ toward SO₂ and H₂O was also studied.

1 Materials and methods

1.1 Preparation of supports and catalysts

Ce-Zr hydroxide was prepared by a co-precipitation method. Ce(NO₃)₃·6H₂O and ZrO(NO₃)₂·2H₂O were used as precursors and were dissolved in distilled water with the molar ratio of 1:1. An aqueous solution of ammonia was used as the precipitator and was added dropwise in the metal salt solution until the pH rose to 10. The resulting precipitates were stirred for 3 hr and then aged for 1 hr, and finally filtered, washed, and dried at 80°C overnight. Ce and Zr hydroxides were prepared with the same process, and used Ce(NO₃)₃·6H₂O and ZrO(NO₃)₂·2H₂O as precursors, respectively.

Mn-base catalysts were prepared by impregnating the support powders of Ce, Zr and Ce-Zr hydroxides with Mn(NO₃)₂ solution for 12 hr, and the molar ratio of Mn/(Ce+Zr) was 0.6:1. Then the samples were dried at 80°C overnight and at 110°C for 6 hr, and finally were calcined at 500°C for 6 hr. The catalysts included Mn/CeO₂, Mn/ZrO₂ and Mn/Ce-ZrO₂.

In order to obtain CeO₂, ZrO₂, and Ce-ZrO₂, some of the hydroxides of Ce, Zr and Ce-Zr were calcined at 500°C for 6 hr. All the chemicals used in the study were of analytic grade.

1.2 Characterization of supports and catalysts

BET surface areas of the catalysts were measured by nitrogen adsorption at -196°C using a NOVA 2000 automated gas sorption system (Quantachrome Instruments, USA). The pore size distribution was calculated from the desorption branch of the N₂ adsorption isotherm using the Barrett-Joyner-Halenda (BJH) formula.

Powder X-ray diffraction (XRD) measurements were performed on a Rigaku D/Max 2500 system using Cu K α radiation (40 kV, 100 mA) (Rigaku Corporation, Japan).

X-ray photoelectron spectroscopy (XPS) was performed using a Kratos Axis Ultra DLD spectrometer equipped with monochromated Al K α radiation (1486.6 eV) (Shimadzu, Japan). Sample charging effects were eliminated by correcting the observed spectra with the C 1s binding energy value of 284.6 eV. The normal operating pressure in the analysis chamber was controlled to 10⁻⁹ Pa during the measurement.

The temperature-programmed desorption of ammonia (NH₃-TPD) was performed on a tp-5080 automated chemisorption analyzer using 0.1 g catalyst. The powder catalyst was first pretreated in a flow of N₂ (30 mL/min) at 500°C for 1 hr. Subsequently, the sample was cooled down to room temperature and saturated with a stream of pure NH₃ for 30 min (total flow rate = 1 mL/min (STP)). After saturation, the sample was flushed in a pure N₂ flow for 30 min at 100°C. Finally, the sample was heated up to 500°C with a heating rate of 10°C/min. The amount of NH₃ desorption from the catalysts was quantified by a thermal conductivity detector (TCD).

Hydrogen temperature-programmed reduction (H₂-TPR) was performed in the same instrument as the NH₃-TPD using 0.1 g catalyst. The sample was first pretreated in N₂ (30 mL/min) at 500°C for 1 hr and then cooled to room temperature. Subsequently, the sample was heated up to 900°C at a rate of 10°C/min under 5 vol.% H₂/N₂. The consumption of H₂ was measured by a TCD.

FT-IR spectra were acquired with a Nicolet Magna-560 FT-IR spectrometer using a thin self-supporting sample wafer accumulation of 100 scans running at 4 cm⁻¹ resolution.

Thermo gravimetric analyses (TGA) were performed on 0.01 g of sample with a NETZSCH Thermal Analysis System under a nitrogen flow of 20 mL/min, using a heating rate of 10°C/min from room temperature to 900°C (NETZSCH Corporation, Germany).

1.3 Catalytic activity test

The SCR activity measurement was performed in a fixed-bed flow reactor. The concentrations of simulated gases were as follows: 600 ppm NO, 660 ppm NH₃, 6 vol.% O₂, 3 vol.% H₂O (when used), 100 ppm SO₂ (when used) and N₂ as balance gas. In all the runs, the total gas flow rate was maintained at 300 mL/min over 0.5 g catalyst and GHSV was about 45,000 hr⁻¹. The feed gases were mixed and preheated in a chamber before entering the reactor. The water vapor was generated by passing N₂ through a gas-washing bottle containing deionized water at different heating temperatures. During the measurements, the concentrations of NO at the inlet and outlet of the reactor were monitored by a flue gas analyzer (KM900/KM9106, Kane International Ltd., United Kingdom). The NO conversion

was calculated using the following equation:

$$\text{NO conversion} = \frac{\text{NO}_{\text{in}} - \text{NO}_{\text{out}}}{\text{NO}_{\text{in}}} \times 100\% \quad (1)$$

where, NO_{in} (ppm) is the inlet NO_x concentration; NO_{out} (ppm) is the outlet NO_x concentration.

2 Results and discussion

2.1 Catalyst characterization

The BET surface area, pore volume, and pore size of different samples are summarized in **Table 1**. The BET surface areas of CeO₂, ZrO₂ and Ce-ZrO₂ were 49.85, 45.93 and 69.77 m²/g, respectively, which indicated that the mixture of Ce and Zr could increase the surface area. This was mainly because Zr⁴⁺ could improve the thermal stability of CeO₂ and inhibit the sintering of CeO₂ during the combustion process (Wu et al., 2008). The surface areas of Mn/ZrO₂ and Mn/Ce-ZrO₂ were larger than those of ZrO₂ and Ce-ZrO₂. In some reports, surface areas of catalysts were smaller than those of the supports (Zhang et al., 2011; Ko et al., 2012) because the free pores of the support were partially occupied during the impregnation process. In the present work, hydroxides were used as catalyst supports, and some interaction between hydroxides and Mn might occur during the impregnation process. The BET surface area of Mn/CeO₂ was smaller than that of CeO₂, which indicated that the interaction between Mn and Ce could be ignored.

The XRD patterns of the catalysts are shown in **Fig. 1**. The diffraction peaks of Mn/ZrO₂ were attributed to Mn₂O₃ and ZrO₂ and the diffraction peaks of Mn/CeO₂ and Mn/Ce-ZrO₂ were attributed to Mn₂O₃ and CeO₂. CeO₂ diffraction peaks in Mn/Ce-ZrO₂ were broader than in Mn/CeO₂ due to the poorer crystallinity of CeO₂ in Mn/Ce-ZrO₂. Furthermore, ZrO₂ diffraction peaks could not be detected in Mn/Ce-ZrO₂, which might be due to the amorphous state of ZrO₂, the strong background of CeO₂ or the incorporation of Zr in the ceria lattice (Fornasiero et al., 1995). In all of the three catalysts, Mn₂O₃ was the only crystal phase of manganese oxides that could be detected. The Scherrer Formula was used to calculate the grain size of Mn₂O₃ in Mn/ZrO₂, Mn/CeO₂ and Mn/Ce-ZrO₂, and the results were 305, 212 and 180 Å, respectively. These results suggested that Mn/Ce-ZrO₂ had the best manganese

Table 1 BET analysis results of various catalysts

Sample	BET surface area (m ² /g)	Pore volume (cm ³ /g)	Pore size (nm)
CeO ₂	49.85	0.0642	4.07
ZrO ₂	45.93	0.1127	7.43
Ce-ZrO ₂	69.77	0.0816	3.62
Mn/CeO ₂	38.20	0.0940	7.78
Mn/ZrO ₂	129.76	0.1976	4.66
Mn/Ce-ZrO ₂	96.50	0.1524	4.78

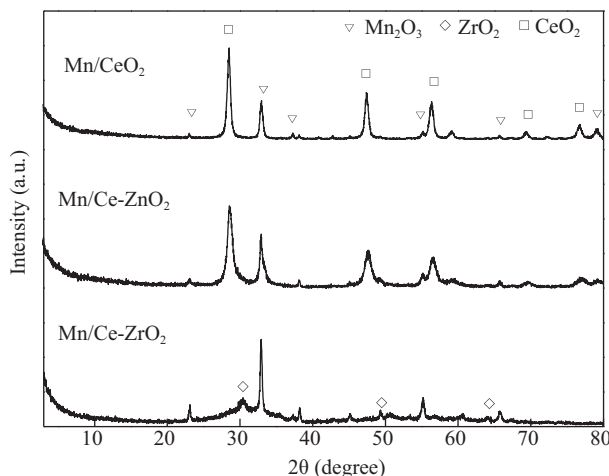


Fig. 1 XRD patterns of different catalysts.

oxide dispersion. This was consistent with a report (Lee et al., 2012) which pointed out that the introduction of Ce into the catalyst improved the manganese dispersion.

H₂-TPR analysis was conducted in the present study to investigate the redox behavior of the three catalysts. As shown in **Fig. 2**, three reduction peaks were detected in every sample, and the number in the figure represents the temperature at the peak center. The reduction temperatures of Mn/CeO₂ shifted towards lower temperature compared to those of Mn/ZrO₂ and Mn/Ce-ZrO₂, indicating that Mn/CeO₂ was more easily reduced. The low temperature peak area of Mn/Ce-ZrO₂ was much larger than that of Mn/ZrO₂ and Mn/CeO₂, suggesting that Mn/Ce-ZrO₂ had more reductive species at low temperature. Therefore, Mn/CeO₂ and Mn/Ce-ZrO₂ have better redox properties.

According to the previous reports (Ko et al., 2012; Azalim et al., 2011; Wei et al., 2012), the reduction peak positions of CeO₂, ZrO₂ and Ce-ZrO₂ were different from those of Mn/CeO₂, Mn/ZrO₂ and Mn/Ce-ZrO₂. Furthermore, it was reported that the reduction peaks of MnO_x in Mn/TiO₂ were centered at 303, 392 and 463°C (Thirupathi and Smiriotis, 2011; 2011) and they

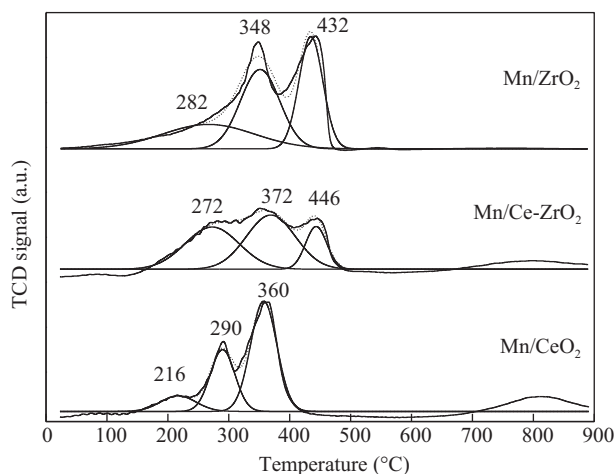


Fig. 2 Temperature-programmed reduction profiles of different catalysts.

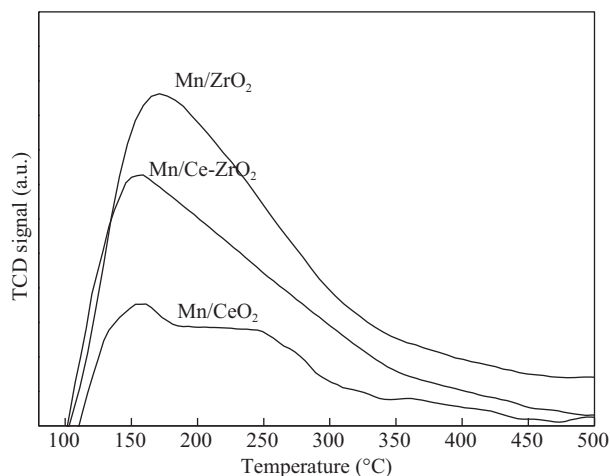


Fig. 3 Temperature-programmed desorption profiles of different catalysts.

were also different from those of Mn/CeO₂, Mn/ZrO₂ and Mn/Ce-ZrO₂. These results indicated that there might be interaction between the catalyst support and the active component. Due to the interaction of different components in the catalysts, the reduction peaks could not be attributed to the reduction of a single component but the combined reduction of different components.

NH₃-TPD analysis was carried out to measure the surface acidity of the three catalysts. As shown in **Fig. 3**, the shapes of the NH₃-TPD patterns of the three samples were similar. Only one broad desorption peak was detected in the experiment, which spanned the temperature range from 100 to 450°C. The peak could be assigned to the successive desorption of ammonia physically adsorbed to weak acid sites (100–220°C) and strong acid sites (220–440°C), which was similar to a previous report (Mhamdi et al., 2009). The NH₃ desorption peak of Mn/CeO₂ was very weak, because cerium oxides could hardly give any contribution to NH₃ adsorption (Shen et al., 2009). With the introduction of Zr into the support, the bound NH₃ uptake increased significantly, suggesting that Zr gave rise to more acid sites for the catalysts.

XPS analyses were carried out to investigate the chemical states and atom concentration on the surface of catalysts. **Figure 4** shows the Mn 2p, O 1s, Zr 3d and Ce 3d photoelectron peaks of the catalysts measured by XPS. The Mn 2p photoelectron peaks of Mn/CeO₂ were very broad. A significant increase in the intensity and sharpening of Mn 2p peaks could be noted when Zr was introduced in Mn/Ce-ZrO₂, and Mn/ZrO₂ had the most intense Mn 2p

peaks. This suggested that the surface atom concentration of Mn for Mn/ZrO₂ was higher than that for the other two catalysts. Mn 2p_{3/2} spectra of the catalysts were composed of two overlapping peaks around the BE of 643.5 and 641.2 eV due to Mn⁴⁺ and Mn³⁺, respectively (Qi and Yang, 2004; Thirupathi and Smirniotis, 2012). All peaks of the catalysts around 641.2 eV were sharper than those around 643.5 eV, indicating that Mn₂O₃ was a major phase and MnO₂ was a minor phase in the catalysts. Only the crystal pattern of Mn₂O₃ could be detected in the catalysts from the XRD analysis, but the XPS analysis showed the co-existence of Mn₂O₃ and MnO₂ on the surface of the catalysts. Thus the MnO₂ in the three catalysts might be amorphous.

O 1s spectra of the samples were composed of two overlapping peaks. The first peak in the range of 529.5–530.5 eV (O_β) was due to the lattice oxygen (Larachi et al., 2002; Carja et al., 2007; Yu et al., 2010) and the second peak in the range of 531.3–531.7 eV (O_α) corresponded to the weakly surface-adsorbed oxygen (Tejuca and Fierro, 1989; Qin et al., 2007). O_β shifted towards higher BE when Zr was introduced. This might due to the higher BE of lattice oxygen in ZrO₂ than that in CeO₂. Meanwhile, the O_α area of Mn/CeO₂ and Mn/Ce-ZrO₂ was larger than that of Mn/ZrO₂ due to more weakly adsorbed species on the surface of Mn/CeO₂ and Mn/Ce-ZrO₂. As reported previously, gas phase oxygen participated in the SCR reaction by filling the oxygen vacancies over the catalyst surface (Ettireddy et al., 2012), and the surface-adsorbed oxygen favored SCR activity (Wu et al., 2008). The BE of Zr 3d was similar in Mn/Ce-ZrO₂ and Mn/ZrO₂ and the BE of Ce 3d was similar in Mn/Ce-ZrO₂ and Mn/CeO₂. Therefore, it could be concluded that the mixture of Zr and Ce in Mn/Ce-ZrO₂ did not change the BE of Zr and Ce very much.

The surface atom percentage of catalysts and atomic ratio of Mn/(Ce+Zr) are shown in **Table 2**. The overall ratio of Ce/Zr for Mn/Ce-ZrO₂ was 1, but it was 7.5 on the surface of Mn/Ce-ZrO₂, which indicated that Ce was more easily accumulated on the surface of Mn/Ce-ZrO₂ than Zr. The Mn concentration on the surface of Mn/ZrO₂ was much higher than that on the surface of Mn/CeO₂ and Mn/Ce-ZrO₂, suggesting that Zr caused Mn to accumulate on the surface of the catalysts. This might be the reason for the sharp diffraction peaks of Mn₂O₃ in Mn/ZrO₂ (**Fig. 1**). The enrichment of Mn and Ce on the surface of the catalysts resulted in the higher ratio of Mn/(Ce+Zr) for Mn/ZrO₂ than that for Mn/CeO₂ and Mn/Ce-ZrO₂. This

Table 2 Surface atom percentage and the ratio of Mn/(Ce+Zr) of different catalysts determined from XPS

Sample	Surface atom percentage (%)						Mn/(Ce+Zr)
	Ce	Zr	Mn ³⁺	Mn ⁴⁺	O _α	O _β	
Mn/CeO ₂	24.14	0	3.39	2.98	56.61	12.88	0.26
Mn/Ce-ZrO ₂	21.41	2.84	4.69	3.52	43.57	23.97	0.34
Mn/ZrO ₂	0	9.47	14.48	8.18	14.65	53.22	2.39

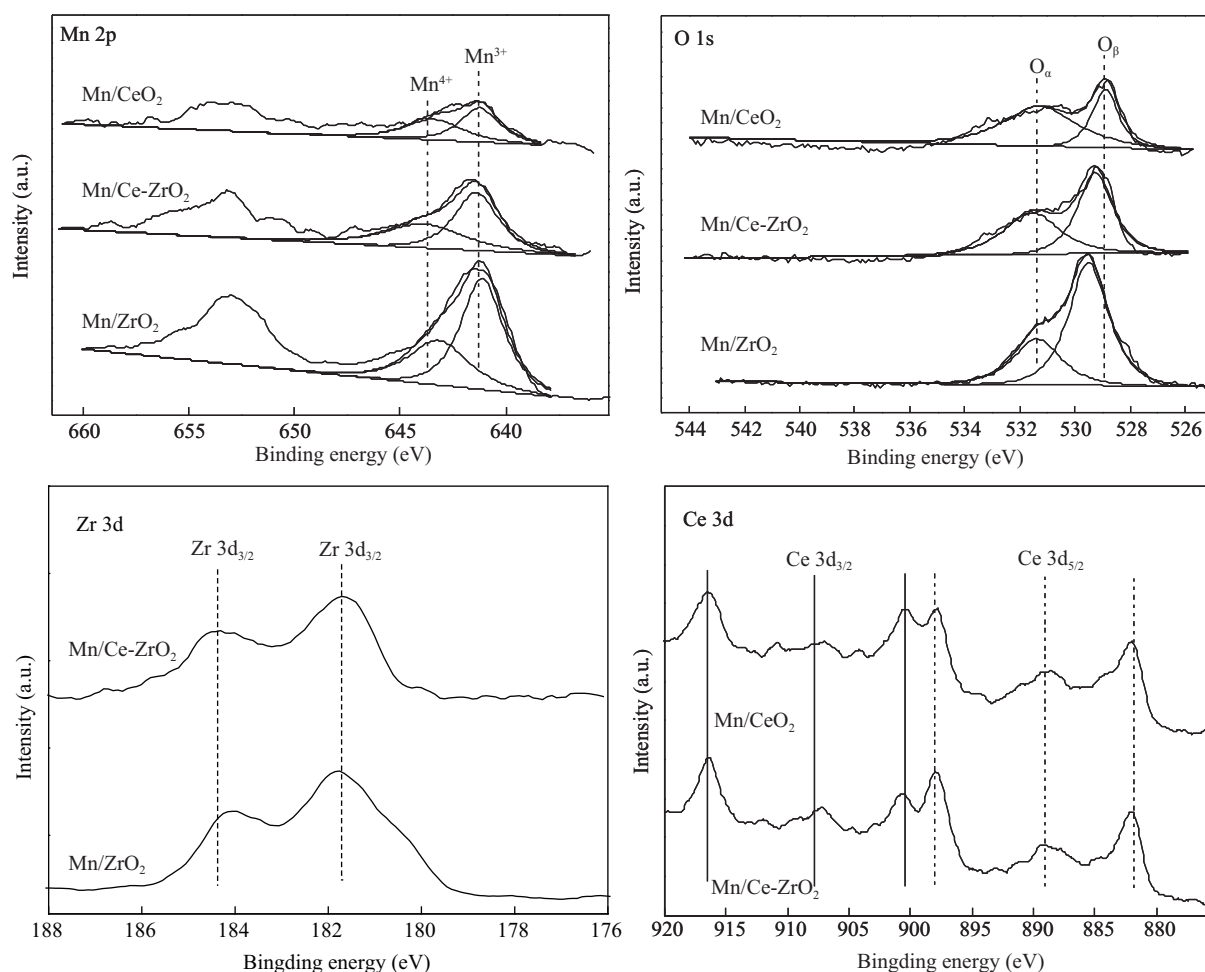


Fig. 4 XPS spectra of Mn 2p, O 1s, Zr 3d and Ce 3d for different catalysts.

was in agreement with the literature of Ettireddy et al. (2007) which studied Mn-based TiO₂-supported catalysts and found that the surface atom ratio of Mn/Ti increased significantly at higher Mn loading, due to the formation of microcrystalline Mn oxide species on the catalyst surface. O_α was much higher and O_β was much lower in Mn/CeO₂ and Mn/Ce-ZrO₂ than that in Mn/ZrO₂, suggesting that the introduction of Ce increased the amount of O_α in Mn/Ce-ZrO₂.

2.2 SCR catalytic activity

The effect of manganese loading on SCR activity is shown in Fig. 5a. The activity of the Ce-ZrO₂ support was very low (less than 25%, data not shown). After the addition of Mn, the activities of the catalysts increased sharply, which suggested that Mn species played a significant role in this reaction. This was consistent with the report of Qi and Yang (2003) concerning the MnO_x/TiO₂ catalyst. With the increase of the loading amount of Mn, the SCR activity increased first and then decreased, and the maximum activity value occurred when the temperature reached 180°C. At all of the reaction temperatures, the optimal value for Mn/(Ce+Zr) was 0.6. Therefore, 0.6 was

chosen as the ratio of Mn/(Ce+Zr) in later experiments.

The catalytic activities of Mn/CeO₂, Mn/Ce-ZrO₂ and Mn/ZrO₂ for low-temperature SCR were measured in the temperature range from 100 to 220°C and the results are shown in Fig. 5b. The activity of Mn/CeO₂ and Mn/Ce-ZrO₂ was higher than that of Mn/ZrO₂. Characterization results showed that Mn/ZrO₂ had the largest BET surface area and the strongest surface acidity, while Mn/ZrO₂ had the worst dispersion of manganese oxides, the weakest reductive capability and the least adsorbed oxygen species on its surface. Therefore, combined with the characterization results and the results of the catalytic activities, the dispersion of manganese oxides, the reductive capability and the adsorbed oxygen species on the surface of the catalysts were the determinants of catalytic activity. This was consistent with previous reports. The reports pointed out that the dispersion of the manganese oxide played an important role in the formation of amorphous-phase manganese oxide, which had good performance in the SCR reaction (Kijlstra et al., 1997; Kapteijn et al., 1994; Huang and Yang, 2001). In the meantime, a strong reductive capability of catalysts and oxygen ions on the surface of catalysts promoted the catalytic activity (Wu et al.,

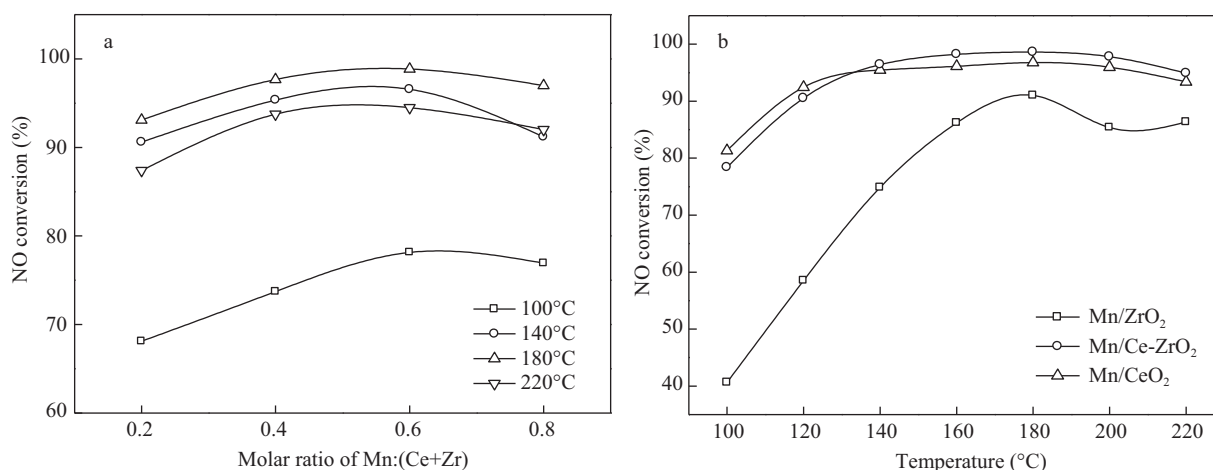


Fig. 5 NO conversion over different catalysts with different MnO_x loading (a) and over different catalysts (b).

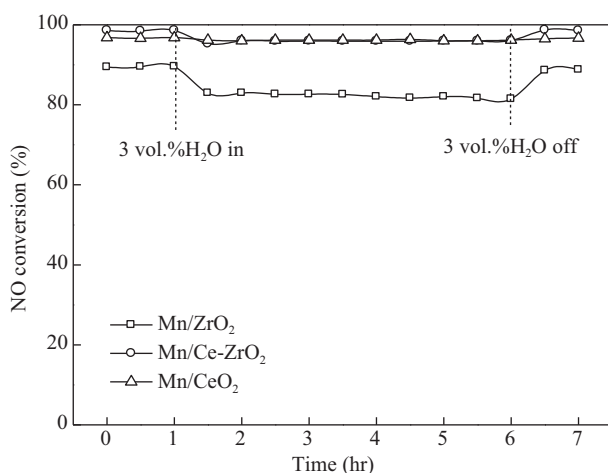


Fig. 6 Effect of H₂O on NO conversion over different catalysts at 180°C.

2008; Liu et al., 2007). For all of the three catalysts, the maximum activity value appeared at 180°C, being 98.6%, 96.8% and 91.0% for Mn/Ce-ZrO₂, Mn/CeO₂ and Mn/ZrO₂, respectively.

2.3 Effect of H₂O on SCR catalytic activity

In order to evaluate the resistance to H₂O of all the catalysts, the catalysts were subjected to a stream of 3 vol.% H₂O at 180°C. As shown in Fig. 6, the activity of Mn/CeO₂ was almost unchanged when H₂O was added. Meanwhile, the activities of Mn/ZrO₂ and Mn/Ce-ZrO₂ slightly decreased from 89.5% and 98.6% to 82.9% and 95.3% with the addition of H₂O, respectively. After the removal of H₂O, the activities of Mn/ZrO₂ and Mn/Ce-ZrO₂ were restored to their original levels. These results showed that these catalysts had good resistance to H₂O and the inhibitory effect of H₂O was reversible for these catalysts. The slight inhibitory effect on catalytic activity could be contributed to the competitive adsorption of H₂O, which blocked active sites available for the adsorption of NH₃ and NO (Amiridis et al., 1996; Tufano and Turco, 1993).

2.4 Effect of H₂O and SO₂ on SCR catalytic activity

There are small amounts of SO₂ remaining in flue gas even after the desulfurizer. Thus it is necessary to investigate the effect of SO₂ + H₂O on SCR activity. Before 3 vol.% H₂O and 100 ppm SO₂ were added, the SCR reaction was stabilized for 1 hr at 180°C. As shown in Fig. 7a, when 3 vol.% H₂O and 100 ppm SO₂ were added into the flue gas, a sharp decline of the NO conversion for Mn/Ce-ZrO₂ from 98.5% to 91.2% was observed in the first hour, and then it nearly stabilized. On the contrary, sustained declines of NO conversions for Mn/CeO₂ and Mn/ZrO₂ were detected over 6 hr, from 96.8% to 61.5% and from 89.5% to 67.1%, respectively. After the removal of SO₂ and H₂O, the activity of Mn/Ce-ZrO₂ almost returned to the original level, from 87.1%, and the activity of Mn/ZrO₂ returned to 79.7%, which was 10% lower than its original level. But the activity of Mn/CeO₂ was almost unchanged. These results revealed that the mixed support of Ce-ZrO₂ used in Mn/Ce-ZrO₂ evidently improved the resistance of the catalyst to SO₂ and H₂O.

The effect of SO₂ and H₂O on NO conversion over Mn/Ce-ZrO₂ at different temperatures (160, 180 and 200°C) are shown in Fig. 7b). Similar NO conversion and resistance to SO₂ and H₂O were observed at 180 and 200°C. The activity measured at 160°C had a faster decline compared with that at 180 and 200°C. However, it still showed a high level of activity for NO conversion (79.4%) even at 160°C. These results showed that the resistance to SO₂ and H₂O for Mn/Ce-ZrO₂ increased with increasing temperature.

2.5 FT-IR spectra and TGA for the catalysts

FT-IR analyses were performed in order to investigate formation of sulfate on the catalysts, and the results are shown in Fig. 8. Compared to the fresh catalysts, a new peak appeared at 1104 or 1106 cm⁻¹, which was attributed to free SO₄²⁻ for all the used catalysts of Mn/Ce-ZrO₂, Mn/ZrO₂ and Mn/CeO₂ (Huang et al., 2008). Meanwhile,

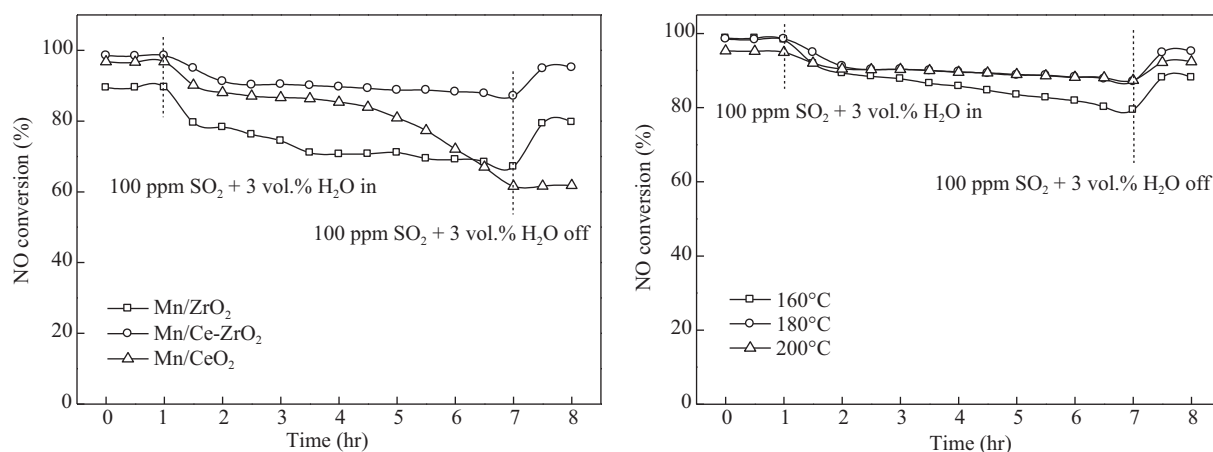


Fig. 7 Effect of H₂O and SO₂ on NO conversion over different catalysts at 180°C (a) and over Mn/Ce-ZrO₂ catalyst at different temperatures (b).

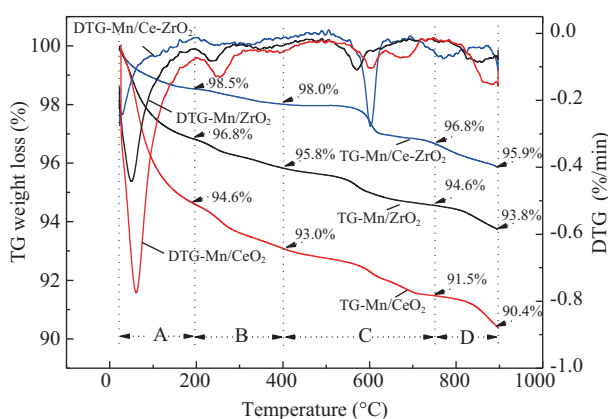


Fig. 9 TGA of the catalysts after 6 hr treatment with H₂O and SO₂.

the peaks at 1373, 1379 or 1382 cm⁻¹ arising from the nitrate species spectrum (Huang and Yang, 2001) were clearly larger in the used catalysts than those in the fresh ones. The peaks in the fresh catalysts could be attributed to incompletely decomposed Mn(NO₃)₂. Previous reports (Madia et al., 2002; Liu and He, 2010) have pointed out that NH₄NO₃ can form on the surface of the catalysts during the reaction process and it could exist stably, because its decomposition temperature is about 200°C. Therefore, the larger peaks in the used catalysts could be attributed to NH₄NO₃ formation during the reaction process. After reaction, Mn/CeO₂ had the sharpest band around 1104 cm⁻¹ but Mn/Ce-ZrO₂ had the weakest band around 1106 cm⁻¹. The result showed that Mn/Ce-ZrO₂ had the weakest sulfation during the reaction process. The poisoning effect of SO₂ on catalysts mainly took place via two approaches: the deposition of ammonium sulfate on the catalyst surface covering available active sites (Huang et al., 2002; Yu et al., 2010; Zhu et al., 2001) and the sulfation of active components resulting in their inactivation (Kijlstra et al., 1997, 1998). Therefore, the weak sulfation of Mn/Ce-ZrO₂ corresponded to its good resistance to SO₂ poisoning.

TGA were performed to distinguish the species of sulfate salts on the surfaces of the used catalysts, and the results are shown in **Fig. 9**. It can be seen that the

weight losses of the used catalysts can be divided into four phases according to the peaks from DTG: A (< 200°C), B (200°C–400°C), C (400–750°C), and D (> 750°C). These four phases can be attributed to the departure of water molecules and hydration, the decomposition of ammonia sulfate and ammonium bisulfate (Mao et al., 2011), the decomposition of cerous sulfate and zirconium sulfate (Strydom and Pretorius, 1993; Poston et al., 2003) and the decomposition of manganese sulfate (Mao et al., 2011), respectively. The weight losses in different phases are shown in **Table 3**. It can be seen that the weight losses corresponding to the dehydration process and the decomposition of sulfates in Mn/Ce-ZrO₂ were much lower than those in Mn/CeO₂. This indicated that there were fewer water molecules and less hydration and sulfate forming on Mn/Ce-ZrO₂ than on Mn/CeO₂. These results agreed well with the outcomes of the resistance to SO₂ and H₂O of Mn/Ce-ZrO₂, Mn/ZrO₂ and Mn/CeO₂.

Table 3 Different weight losses for the used catalysts

Sample	Weight loss resulting from the dehydration process (%)	Weight loss resulting from the decomposition of sulfates (%)		
		Ammonia sulfate	Cerous and zirconium sulfate	Manganese sulfate
Mn/Ce-ZrO ₂	1.5	0.5	1.2	0.9
Mn/ZrO ₂	3.2	1.0	1.2	0.8
Mn/CeO ₂	5.4	1.6	1.5	1.1

3 Conclusions

In this work, CeO₂, ZrO₂ and a mixture of Ce-ZrO₂ were used to support manganese oxides. It was found that Mn/Ce-ZrO₂ and Mn/CeO₂ have better low-temperature activities than Mn/ZrO₂. This was mainly due to the higher dispersion of manganese oxides, better redox character and more surface adsorbed oxygen of Mn/Ce-ZrO₂ and Mn/CeO₂ compared to Mn/ZrO₂. Furthermore, Mn/Ce-ZrO₂ had better resistance to SO₂ and H₂O due to the weak

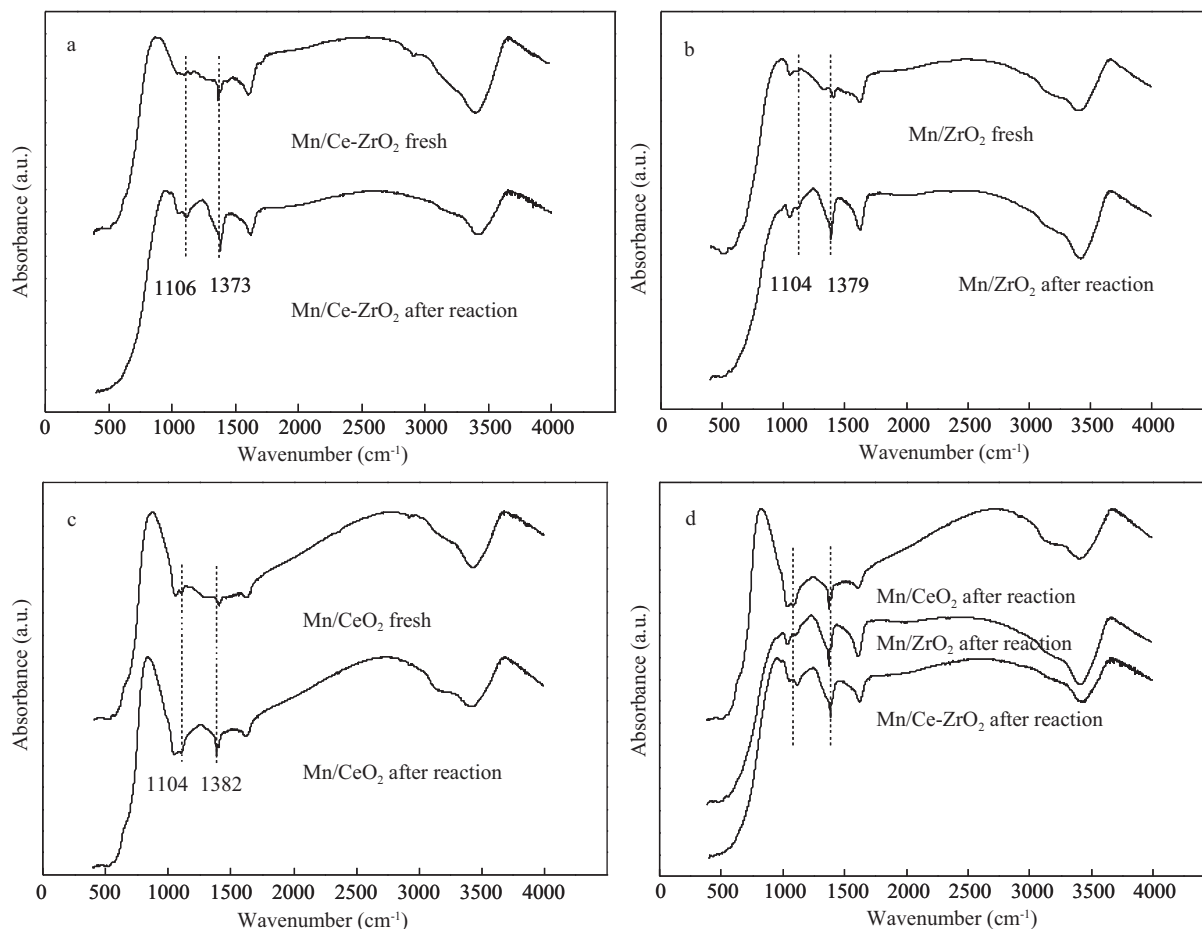


Fig. 8 FT-IR spectrum of the catalysts before and after 6 hr treatment with H₂O and SO₂.

water absorption and weak sulfation process on the surface of the catalyst.

Acknowledgments

This work was supported by the National Natural Science Foundation of China (No. 51176077, 50976050), and the Tianjin Municipal Natural Science Foundation Project (No. 12JCZDJC29300).

References

- Amiridis M D, Wachs I E, Deo G, Jehng J M, Kim D S, 1996. Reactivity of V₂O₅ catalysts for the selective catalytic reduction of NO by NH₃: Influence of vanadia loading, H₂O, and SO₂. *Journal of Catalysis*, 161(1): 247–253.
- Azalim S, Franco M, Brahmī R, Giraudon J M, Lamonier J F, 2011. Removal of oxygenated volatile organic compounds by catalytic oxidation over Zr-Ce-Mn catalysts. *Journal of Hazardous Materials*, 188(1-3): 422–427.
- Baidya T, Gupta A, Deshpandey P A, Madras G, Hegde M S, 2009. High oxygen storage capacity and high rates of CO oxidation and NO reduction catalytic properties of Ce_{1-x}Sn_xO₂ and Ce_{0.78}Sn_{0.2}Pd_{0.02}O_{2-δ}. *The Journal of Physical Chemistry C*, 113(10): 4059–4068.
- Bröer S, Hammer T, 2000. Selective catalytic reduction of nitrogen oxides by combining a non-thermal plasma and a V₂O₅-WO₃/TiO₂ catalyst. *Applied Catalysis B: Environmental*, 28(2): 101–111.
- Carja G, Kameshima Y, Okada K, Madhusoodana C D, 2007. Mn-Ce/ZSM₅ as a new superior catalyst for NO reduction with NH₃. *Applied Catalysis B: Environmental*, 73(1-2):60–64.
- Casapu M, Krocher O, Elsener M, 2009. Screening of doped MnO_x-CeO₂ catalysts for low-temperature NO-SCR. *Applied Catalysis B: Environmental*, 88(3-4): 413–419.
- Chary K V R, Kumar C P, Naresh D, Bhaskar T, Sakata Y, 2006. Characterization and reactivity of Al₂O₃-ZrO₂ supported vanadium oxide catalysts. *Journal of Molecular Catalysis A: Chemical*, 243(2): 149–157.
- Chen Z H, Wang F R, Li H, Yang Q, Wang L F, Li X H, 2012. Low-temperature selective catalytic reduction of NO_x with NH₃ over Fe-Mn mixed-oxide catalysts containing Fe₃Mn₃O₈ phase. *Industrial & Engineering Chemistry Research*, 51(1): 202–212.
- Choo S T, Yim S D, Nam I S, Ham S W, Lee J B, 2003. Effect of promoters including WO₃ and BaO on the activity and durability of V₂O₅/sulfated TiO₂ catalyst for NO reduction by NH₃. *Applied Catalysis B: Environmental*, 44(3): 237–252.
- Ettireddy P R, Ettireddy N, Boningari T, Pardemann R, Smirniotis P G, 2012. Investigation of the selective catalytic reduction of nitric oxide with ammonia over Mn/TiO₂ catalysts through transient isotopic labeling and in situ FT-

- IR studies. *Journal of Catalysis*, 292: 53–63.
- Ettireddy P R, Ettireddy N, Mamedov S, Boolchand P, Smirniotis P G, 2007. Surface characterization studies of TiO₂ supported manganese oxide catalysts for low temperature SCR of NO with NH₃. *Applied Catalysis B: Environmental*, 76(1-2): 123–134.
- Fornasiero P, Dimonte R, Rao G R, Kaspar J, Meriani S, Trovarelli A et al., 1995. Rh-loaded CeO₂-ZrO₂ solid-solutions as highly efficient oxygen exchangers: dependence of the reduction behavior and the oxygen storage capacity on the structural-properties. *Journal of Catalysis*, 151(1): 168–177.
- Huang H Y, Yang R T, 2001. Removal of NO by reversible adsorption on Fe-Mn based transition metal oxides. *Langmuir*, 17(16): 4997–5003.
- Huang J H, Tong Z Q, Huang Y, Zhang J F, 2008. Selective catalytic reduction of NO with NH₃ at low temperatures over iron and manganese oxides supported on mesoporous silica. *Applied Catalysis B: Environmental*, 78(3-4): 309–314.
- Huang Z G, Zhu Z P, Liu Z Y, 2002. Combined effect of H₂O and SO₂ on V₂O₅/AC catalysts for NO reduction with ammonia at lower temperatures. *Applied Catalysis B: Environmental*, 39(4): 361–368.
- Kapteijn F, Singoredjo L, Andreini A, Moulijn J A, 1994. Activity and selectivity of pure manganese oxides in the selective catalytic reduction of nitric oxide with ammonia. *Applied Catalysis B: Environmental*, 3(2-3): 173–189.
- Kašpar J, Fornasiero P, Hickey N, 2003. Automotive catalytic converters: current status and some perspectives. *Catalysis Today*, 77(4): 419–449.
- Kijlstra W S, Biervliet M, Poels E K, Blik A, 1998. Deactivation by SO₂ of MnOx/Al₂O₃ catalysts used for the selective catalytic reduction of NO with NH₃ at low temperatures. *Applied Catalysis B: Environmental*, 16(4): 327–337.
- Kijlstra W S, Brands D S, Smit H I, Poels E K, Blik A, 1997. Mechanism of the selective catalytic reduction of NO with NH₃ over MnOx/Al₂O₃: II. Reactivity of adsorbed NH₃ and NO complexes. *Journal of Catalysis*, 171(1): 219–230.
- Ko J H, Park S H, Jeon J K, Kim S S, Kim S C, Kim J M et al., 2012. Low temperature selective catalytic reduction of NO with NH₃ over Mn supported on Ce_{0.65}Zr_{0.35}O₂ prepared by supercritical method: Effect of Mn precursors on NO reduction. *Catalysis Today*, 185(1): 290–295.
- Larachi F, Pierre J, Adnot A, Bernis A, 2002. Ce 3d XPS study of composite Ce_xMn_{1-x}O_{2-y} wet oxidation catalysts. *Applied Surface Science*, 195(1-4): 236–250.
- Lee S M, Park K H, Hong S C, 2012. MnOx/CeO₂-TiO₂ mixed oxide catalysts for the selective catalytic reduction of NO with NH₃ at low temperature. *Chemical Engineering Journal*, 195-196: 323–331.
- Liu F D, He H, 2010. Selective catalytic reduction of NO with NH₃ over manganese substituted iron titanate catalyst: Reaction mechanism and H₂O/SO₂ inhibition mechanism study. *Catalysis Today*, 153(3-4): 70–76.
- Liu Z M, Wang K C, Zhang X Y, Wang J L, Cao H Y, Gong M C et al., 2009. Study on methane selective catalytic reduction of NO on Pt/Ce_{0.67}Zr_{0.33}O₂ and its application. *Journal of Natural Gas Chemistry*, 18(1): 66–70.
- Liu Z M, Wang R L, Zhong J B, Chen Y Q, Yan S H, Gong M C, 2007. Catalytic combustion of toluene over platinum supported on Ce-Zr-O solid solution modified by Y and Mn. *Journal of Hazardous Materials*, 149(3): 742–746.
- Madia G, Koebel M, Elsener M, Wokaun A, 2002. Side reactions in the selective catalytic reduction of NO_x with various NO₂ fractions. *Industrial & Engineering Chemistry Research*, 41(16): 4008–4015.
- Mao L Q, T-Raissi A, Huang C P, Muradov N Z, 2011. Thermal decomposition of (NH₄)₂SO₄ in presence of Mn₃O₄. *International Journal of Hydrogen Energy*, 36(10): 5822–5827.
- Marbán G, Fuertes A B, 2001. Low-temperature SCR of NO_x with NH₃ over Nomex™ rejects-based activated carbon fibre composite-supported manganese oxides: Part I. Effect of pre-conditioning of the carbonaceous support. *Applied Catalysis B: Environmental*, 34(1): 43–53.
- Mhamdi M, Khaddar-Zine S, Ghorbel A, 2009. Influence of the cobalt salt precursors on the cobalt speciation and catalytic properties of H-ZSM-5 modified with cobalt by solid-state ion exchange reaction. *Applied Catalysis A: General*, 357(1): 42–50.
- Peña D A, Uphade B S, Smirniotis P G, 2004. TiO₂-supported metal oxide catalysts for low-temperature selective catalytic reduction of NO with NH₃: I. Evaluation and characterization of first row transition metals. *Journal of Catalysis*, 221(2): 421–431.
- Poston J A, Siriwardane R V, Fisher E P, Miltz A L, 2003. Thermal decomposition of the rare earth sulfates of cerium(III), cerium(IV), lanthanum(III) and samarium(III). *Applied Surface Science*, 214(1-4): 83–102.
- Qi G S, Yang R T, 2003. Low-temperature selective catalytic reduction of NO with NH₃ over iron and manganese oxides supported on titania. *Applied Catalysis B: Environmental*, 44(3): 217–225.
- Qi G S, Yang R T, 2004. Characterization and FTIR studies of MnOx-CeO₂ catalyst for low-temperature selective catalytic reduction of NO with NH₃. *The Journal of Physical Chemistry B*, 108(40): 15738–15747.
- Qin C L, Oak J J, Ohtsu N, Asami K, Inoue A, 2007. XPS study on the surface films of a newly designed Ni-free Ti-based bulk metallic glass. *Acta Materialia*, 55(6): 2057–2063.
- Reddy B M, Khan A, Yamada Y, Kobayashi T, Loidant S, Volta J C, 2003. Structural characterization of CeO₂-TiO₂ and V₂O₅/CeO₂-TiO₂ catalysts by Raman and XPS techniques. *Journal of Physical Chemistry B*, 107(22): 5162–5167.
- Shen B X, Yao Y, Ma H Q, Liu T, 2011. Ceria modified MnOx/TiO₂-Pillared clays catalysts for the selective catalytic reduction of NO with NH₃ at low temperature. *Chinese Journal of Catalysis*, 32(11-12): 1803–1811.
- Shen Y S, Zhu S M, Qiu T, Shen S B, 2009. A novel catalyst of CeO₂/Al₂O₃ for selective catalytic reduction of NO by NH₃. *Catalysis Communications*, 11(1): 20–23.
- Smirniotis P G, Peña D A, Uphade B S, 2001. Low-temperature selective catalytic reduction (SCR) of NO with NH₃ by using Mn, Cr, and Cu oxides supported on Hombikat TiO₂. *Angewandte Chemie International Edition*, 40(13): 2479–2481.
- Strydom C A, Pretorius G, 1993. The thermal decomposition of zirconium sulphate hydrate. *Thermochimica Acta*, 223(28): 223–232.
- Tang X L, Hao J M, Yi H H, Li J H, 2007. Low-temperature SCR

- of NO with NH₃ over AC/C supported manganese-based monolithic catalysts. *Catalysis Today*, 126(3-4): 406–411.
- Tejuca L G, Fierro J L G, 1989. XPS and TPD probe techniques for the study of LaNiO₃ perovskite oxide. *Thermochimica Acta*, 147(2): 361–375.
- Thirupathi B, Smirniotis P G, 2011a. Co-doping a metal (Cr, Fe, Co, Ni, Cu, Zn, Ce, and Zr) on Mn/TiO₂ catalyst and its effect on the selective reduction of NO with NH₃ at low-temperatures. *Applied Catalysis B: Environmental*, 110: 195–206.
- Thirupathi B, Smirniotis P G, 2011b. Effect of nickel as dopant in Mn/TiO₂ catalysts for the low-temperature selective reduction of NO with NH₃. *Catalysis Letters*, 141(10): 1399–1404.
- Thirupathi B, Smirniotis P G, 2012. Nickel-doped Mn/TiO₂ as an efficient catalyst for the low-temperature SCR of NO with NH₃: Catalytic evaluation and characterizations. *Journal of Catalysis*, 288: 74–83.
- Tufano V, Turco M, 1993. Kinetic modelling of nitric oxide reduction over a high-surface area V₂O₅-TiO₂ catalyst. *Applied Catalysis B: Environmental*, 2(1): 9–26.
- Wallin M, Forser S, Thormahlen P, Skoglundh M, 2004. Screening of TiO₂-supported catalysts for selective NO_x reduction with ammonia. *Industrial & Engineering Chemistry Research*, 43(24): 7723–7731.
- Wei Y C, Liu J, Zhao Z, Duan A J, Jiang G Y, 2012. The catalysts of three-dimensionally ordered macroporous Ce_{1-x}Zr_xO₂-supported gold nanoparticles for soot combustion: The metal-support interaction. *Journal of Catalysis*, 287: 13–29.
- Wu Q Y, Chen J X, Zhang J Y, 2008a. Effect of yttrium and praseodymium on properties of Ce_{0.75}Zr_{0.25}O₂ solid solution for CH₄-O₂ reforming. *Fuel Processing Technology*, 89(11): 993–999.
- Wu Z B, Jin R B, Liu Y, Wang H Q, 2008b. Ceria modified MnO_x/TiO₂ as a superior catalyst for NO reduction with NH₃ at low-temperature. *Catalysis Communications*, 9(13): 2217–2220.
- Yu J, Guo F, Wang Y L, Zhu J H, Liu Y Y, Su F B et al., 2010. Sulfur poisoning resistant mesoporous Mn-base catalyst for low-temperature SCR of NO with NH₃. *Applied Catalysis B: Environmental*, 95(1-2): 160–168.
- Zhang Q L, Qiu C T, Xu H D, Lin T, Lin Z E, Gong M C et al., 2011. Low-temperature selective catalytic reduction of NO with NH₃ over monolith catalyst of MnO_x/CeO₂-ZrO₂-Al₂O₃. *Catalysis Today*, 175(1): 171–176.
- Zhu Z P, Liu Z Y, Liu S J, Niu H X, 2001. Catalytic NO reduction with ammonia at low temperatures on V₂O₅/AC catalysts: effect of metal oxides addition and SO₂. *Applied Catalysis B: Environmental*, 30(3-4): 267–276.
- Zhu Z P, Liu Z Y, Liu S J, Niu H X, Hu T D, Liu T et al., 2000. NO reduction with NH₃ over an activated carbon-supported copper oxide catalysts at low temperatures. *Applied Catalysis B: Environmental*, 26(1): 25–35.

Editorial Board of Journal of Environmental Sciences

Editor-in-Chief

Hongxiao Tang Research Center for Eco-Environmental Sciences, Chinese Academy of Sciences, China

Associate Editors-in-Chief

Jiuhui Qu Research Center for Eco-Environmental Sciences, Chinese Academy of Sciences, China
Shu Tao Peking University, China
Nigel Bell Imperial College London, United Kingdom
Po-Keung Wong The Chinese University of Hong Kong, Hong Kong, China

Editorial Board

Aquatic environment

Baoyu Gao
Shandong University, China
Maohong Fan
University of Wyoming, USA
Chihpin Huang
National Chiao Tung University
Taiwan, China
Ng Wun Jern
Nanyang Environment &
Water Research Institute, Singapore
Clark C. K. Liu
University of Hawaii at Manoa, USA
Hokyong Shon
University of Technology, Sydney, Australia
Zijian Wang
Research Center for Eco-Environmental Sciences,
Chinese Academy of Sciences, China
Zhiwu Wang
The Ohio State University, USA
Yuxiang Wang
Queen's University, Canada
Min Yang
Research Center for Eco-Environmental Sciences,
Chinese Academy of Sciences, China
Zhifeng Yang
Beijing Normal University, China
Han-Qing Yu
University of Science & Technology of China

Terrestrial environment

Christopher Anderson
Massey University, New Zealand
Zucong Cai
Nanjing Normal University, China
Xinbin Feng
Institute of Geochemistry,
Chinese Academy of Sciences, China
Hongqing Hu
Huazhong Agricultural University, China
Kin-Che Lam
The Chinese University of Hong Kong
Hong Kong, China
Erwin Klumpp
Research Centre Juelich, Agrosphere Institute
Germany
Peijun Li
Institute of Applied Ecology,
Chinese Academy of Sciences, China

Michael Schloter

German Research Center for Environmental Health
Germany

Xuejun Wang
Peking University, China

Lizhong Zhu
Zhejiang University, China

Atmospheric environment

Jianmin Chen
Fudan University, China
Abdelwahid Mellouki
Centre National de la Recherche Scientifique
France

Yujing Mu
Research Center for Eco-Environmental Sciences,
Chinese Academy of Sciences, China

Min Shao
Peking University, China
James Jay Schauer
University of Wisconsin-Madison, USA

Yuesi Wang
Institute of Atmospheric Physics,
Chinese Academy of Sciences, China

Xin Yang
University of Cambridge, UK

Environmental biology

Yong Cai
Florida International University, USA

Henner Hollert
RWTH Aachen University, Germany

Jaе-Seong Lee
Hanyang University, South Korea

Christopher Rensing
University of Copenhagen, Denmark

Bojan Sedmak
National Institute of Biology, Ljubljana

Lirong Song
Institute of Hydrobiology,
the Chinese Academy of Sciences, China

Chunxia Wang
National Natural Science Foundation of China

Gehong Wei
Northwest A & F University, China

Daqiang Yin
Tongji University, China

Zhongtang Yu
The Ohio State University, USA

Environmental toxicology and health

Jingwen Chen
Dalian University of Technology, China

Jiaying Hu
Peking University, China

Guibin Jiang
Research Center for Eco-Environmental Sciences,
Chinese Academy of Sciences, China

Sijin Liu
Research Center for Eco-Environmental Sciences,
Chinese Academy of Sciences, China

Tsuyoshi Nakanishi
Gifu Pharmaceutical University, Japan

Willie Peijnenburg
University of Leiden, The Netherlands

Bingsheng Zhou
Institute of Hydrobiology,
Chinese Academy of Sciences, China

Environmental catalysis and materials

Hong He
Research Center for Eco-Environmental Sciences,
Chinese Academy of Sciences, China

Junhua Li
Tsinghua University, China

Wenfeng Shangguan
Shanghai Jiao Tong University, China

Yasutake Teraoka
Kyushu University, Japan

Ralph T. Yang
University of Michigan, USA

Environmental analysis and method

Zongwei Cai
Hong Kong Baptist University,
Hong Kong, China

Jiping Chen
Dalian Institute of Chemical Physics,
Chinese Academy of Sciences, China

Minghui Zheng
Research Center for Eco-Environmental Sciences,
Chinese Academy of Sciences, China

Municipal solid waste and green chemistry

Pinjing He
Tongji University, China

Environmental ecology

Rusong Wang
Research Center for Eco-Environmental Sciences,
Chinese Academy of Sciences, China

Editorial office staff

Managing editor Qingcai Feng
Editors Zixuan Wang Suqin Liu Zhengang Mao
English editor Catherine Rice (USA)

JOURNAL OF ENVIRONMENTAL SCIENCES

环境科学学报(英文版)
(<http://www.jesc.ac.cn>)

Aims and scope

Journal of Environmental Sciences is an international academic journal supervised by Research Center for Eco-Environmental Sciences, Chinese Academy of Sciences. The journal publishes original, peer-reviewed innovative research and valuable findings in environmental sciences. The types of articles published are research article, critical review, rapid communications, and special issues.

The scope of the journal embraces the treatment processes for natural groundwater, municipal, agricultural and industrial water and wastewaters; physical and chemical methods for limitation of pollutants emission into the atmospheric environment; chemical and biological and phytoremediation of contaminated soil; fate and transport of pollutants in environments; toxicological effects of terrorist chemical release on the natural environment and human health; development of environmental catalysts and materials.

For subscription to electronic edition

Elsevier is responsible for subscription of the journal. Please subscribe to the journal via <http://www.elsevier.com/locate/jes>.

For subscription to print edition

China: Please contact the customer service, Science Press, 16 Donghuangchenggen North Street, Beijing 100717, China. Tel: +86-10-64017032; E-mail: journal@mail.sciencep.com, or the local post office throughout China (domestic postcode: 2-580).

Outside China: Please order the journal from the Elsevier Customer Service Department at the Regional Sales Office nearest you.

Submission declaration

Submission of an article implies that the work described has not been published previously (except in the form of an abstract or as part of a published lecture or academic thesis), that it is not under consideration for publication elsewhere. The submission should be approved by all authors and tacitly or explicitly by the responsible authorities where the work was carried out. If the manuscript accepted, it will not be published elsewhere in the same form, in English or in any other language, including electronically without the written consent of the copyright-holder.

Submission declaration

Submission of the work described has not been published previously (except in the form of an abstract or as part of a published lecture or academic thesis), that it is not under consideration for publication elsewhere. The publication should be approved by all authors and tacitly or explicitly by the responsible authorities where the work was carried out. If the manuscript accepted, it will not be published elsewhere in the same form, in English or in any other language, including electronically without the written consent of the copyright-holder.

Editorial

Authors should submit manuscript online at <http://www.jesc.ac.cn>. In case of queries, please contact editorial office, Tel: +86-10-62920553, E-mail: jesc@263.net, jesc@rcees.ac.cn. Instruction to authors is available at <http://www.jesc.ac.cn>.

Journal of Environmental Sciences (Established in 1989)

Vol. 25 No. 4 2013

Supervised by	Chinese Academy of Sciences	Published by	Science Press, Beijing, China
Sponsored by	Research Center for Eco-Environmental Sciences, Chinese Academy of Sciences	Distributed by	Elsevier Limited, The Netherlands
Edited by	Editorial Office of Journal of Environmental Sciences P. O. Box 2871, Beijing 100085, China Tel: 86-10-62920553; http://www.jesc.ac.cn E-mail: jesc@263.net , jesc@rcees.ac.cn	Domestic	Science Press, 16 Donghuangchenggen North Street, Beijing 100717, China Local Post Offices through China
Editor-in-chief	Hongxiao Tang	Foreign	Elsevier Limited http://www.elsevier.com/locate/jes
CN 11-2629/X	Domestic postcode: 2-580	Printed by	Beijing Beilin Printing House, 100083, China
		Domestic price per issue	RMB ¥ 110.00

ISSN 1001-0742

